Elsevier Editorial System(tm) for Science of the Total Environment

Manuscript Draft

Manuscript Number:

Title: Selective copper extraction by multi-modified mesoporous silica material, SBA-15

Article Type: VSI: Global CleanUp 2018

Keywords: Mesoporous silica; Amine-grafting; Manganese loading; Adsorption; Copper; Heavy metals

Corresponding Author: Professor Saravanamuthu Vigneswaran, Ph.D.

Corresponding Author's Institution: University of Technology Sydney

First Author: Seongchul Ryu, MSc

Order of Authors: Seongchul Ryu, MSc; Gayathri Naidu, PhD; Hee Moon, PhD; Saravanamuthu Vigneswaran, Ph.D.

Abstract: Selective copper (Cu) recovery from wastewater mitigates environmental pollution and is economically valuable. Mesoporous silica adsorbents with manganese loading and amine-grafting, SBA-15-NH2 and Mn-SBA-15-NH2, were synthesized. The characteristics of the synthesized adsorbents were evaluated in detail in terms of its crystal structure peaks, surface area and pore size distribution, transmission electron microscope and X-ray photoelectron spectroscopy. The results established the high selective Cu adsorption capacity of Mn-SBA-15-NH2 in a mixed heavy metal solution, maintaining 96% competitive adsorption as that of a single Cu solution. Comparatively, Cu adsorption on SBA-15-NH2 decreased by half due to high competition with other heavy metals. Optimal Cu adsorption occurred at pH 5. This pH condition enabled grafted amine group in Mn-SBA-15-NH2 to form strong chelating bonds with Cu, avoiding protonation of amine group (below pH 5) as well as precipitation (above pH 5). The adsorption equilibrium well fitted to Langmuir and Freundlich isotherm models, while kinetic results were represented by models of linear driving force approximation (LDFA) and pore diffusion model (PDM). High regeneration and reuse capacity of Mn-SBA-15-NH2 were well established by its capacity to maintain 90% adsorption capacity in a multiple adsorption-desorption cycle. Cu was selectively extracted from Mn-SBA-15-NH2 with an acid solution.

Suggested Reviewers: Sanghyun Jeong PhD
Research Professor, SungKyunKwan University
sh.jeong@skku.edu
Expert in nanomaterials

Ramesh Thiruvenkatachari PhD
Scientific Officer, Commonwealth Scientific and Industrial Research Organisation (CSIRO)
Ramesh.Thiruvenkatachari@csiro.au
Expert in heavy metal remediation and nanomaterials

Chettiyappan VISVANATHAN PhD
Professor, School of Environment, Resources and Development, Asian Institute of Technology
visu@ait.ac.th
Expert in heavy metal remediation and nanomaterials

Chart Chiemchaisri PhD
Associate Professor, Kasetsart University, Thailand
fengccc@ku.ac.th
Expert in wastewater remediation

Jega Jegatheesan PhD
Professor, School of Chemical and Environmental Engineering, RMIT, Melbourne, Australia
jega.jegatheesan@rmit.edu.au
Expert in resource recovery and mining remediation treatment

Opposed Reviewers:

Cover Letter

Professor S Vigneswaran
Professor of Environmental Engineering
Faculty of Engineering
Main Campus
PO Box 123 Broadway
NSW 2007 Australia
T: +61 2 9514 2641
F: +61 2 9514 2633
s.vigneswaran@uts.edu.au
www.uts.edu.au

UTS CRICOS PROVIDER CODE 00099F

1/05/2019

Prof Ravi Naidu
Guest Editor
Science of the Total Environment

Dear Prof. Ravi,

Please find attached our paper on "**Selective copper extraction by multi-modified mesoporous silica material, SBA-15**" by Seongchul Ryu, Gayathri Naidu, Hee Moon, and Saravanamuthu Vigneswaran for possible publication **in a special issue of the 1st Global CleanUp Congress 2018 in the Science of the Total Environment.** I declare that this paper is the original work of the authors and all the authors agree that it should be submitted to this journal. The manuscript was not previously been submitted to your journal or submitted concurrently to another journal.

The paper abstract is as below

Selective copper (Cu) recovery from wastewater mitigates environmental pollution and is economically valuable. Mesoporous silica adsorbents with manganese loading and amine-grafting, SBA-15-NH_2 and Mn-SBA-15-NH_2 was synthesized. The physical and chemical characteristics of the synthesized adsorbents were evaluated in detail in terms of its crystal structure peaks, surface area and pore size distribution, transmission electron microscope and X-ray photoelectron spectroscopy. The results established the high selective Cu adsorption capacity of Mn-SBA-15-NH_2 in a mixed heavy metal solution, maintaining 96% competitive adsorption as that of a single Cu solution. Comparatively, Cu adsorption on SBA-15-NH_2 decreased by half due to high competition with other heavy metals. Optimal Cu adsorption occurred at pH 5. This pH condition enabled grafted amine group in Mn-SBA-15-NH_2 to form strong chelating bonds with Cu, avoiding protonation of amine group (below pH 5) as well as precipitation (above pH 5). The adsorption equilibrium well fitted to Langmuir and Freundlich isotherm models, while kinetic results were represented by models of linear driving force approximation (LDFA) and pore diffusion model (PDM). High regeneration and reuse capacity of Mn-SBA-15-NH_2 were well established by its capacity to maintain 90% adsorption capacity in a multiple adsorption-desorption cycle. Cu was selectively extracted from Mn-SBA-15-NH_2 with an acid solution.

The authors believe that this paper fits the aim and scope of the journal on total environment, specifically covering the spheres of *hydrosphere and antrosphere*. This is because this study evaluated the potential of remediating acidic mining wastewater (*hydrosphere*) containing heavy metals. Mining wastewater an environmental pollutant that affects the biosphere, hydrosphere, geosphere and anthrosphere. In this study, a green technology (mesoporous silica nanoparticle with high regenerative/reuse capacity) is used to selectively recover copper from the wastewater. Selective recovery of copper with a green technology is a sustainable and economically beneficial approach that can be adopted by the wastewater industry to attain resource recovery, rather than simply treat and dispose of the wastewater (*antrosphere*).

Type of contribution: original research paper.

Yours faithfully,

S Vigneswaran

Title page

Selective copper extraction by multi-modified mesoporous silica material, SBA-15

(1)
Name : Seongchul Ryu
Position: PhD Student
Add: Faculty of Engineering and IT, University of Technology Sydney, P.O. Box 123, Broadway, Ultimo, NSW 2007, Australia
Email: seongchul.ryu@student.uts.edu.au

(2)
Name: Gayathri Naidu
Position: Chancellor's Postdoctoral Research Fellow
Add: Faculty of Engineering and IT, University of Technology Sydney, P.O. Box 123, Broadway, Ultimo, NSW 2007, Australia
Email: gayathri.danasamy@uts.edu.au

(3)
Name : Hee Moon
Position: Professor
Add: School of Chemical Engineering, Chonnam National University, 77 Yongbong-ro, Gwangju 61186, Republic of Korea
Email add: hmoon@chonnam.ac.kr

(4)
Name: Saravanamuthu Vigneswaran
Add: Faculty of Engineering and IT, University of Technology Sydney, P.O. Box 123, Broadway, Ultimo, NSW 2007, Australia
Corresponding author; Email: Saravanamuth.Vigneswaran@uts.edu.au

*Graphical Abstract

Graphical abstract

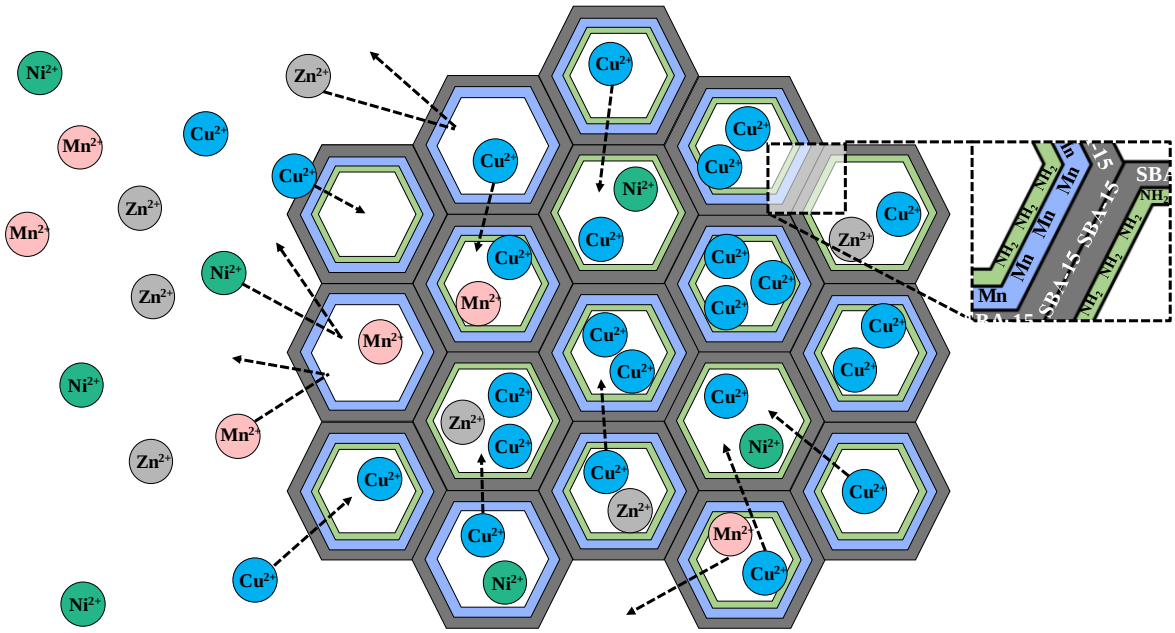

Highlights

- Amine grafted Mn-SBA-15-NH_2 show high Cu adsorption unlike SBA-15-NH_2 and SBA-15.
- Mn-SBA-15-NH_2 maintained 96% selective Cu extraction in mixed heavy metal solution.
- Optimum pH is important for grafted amine group to form complexes with Cu.
- LDFA and PDM models represented kinetics of Cu diffusion satisfactorily.
- Mn-SBA-15-NH_2 maintained 90% adsorption capacity in multiple regeneration cycle

Selective copper extraction by multi-modified mesoporous silica material, SBA-15

Seongchul Ryu[a], Gayathri Naidu[a], Hee Moon[b], Saravanamuthu Vigneswaran[a*],

[a] Faculty of Engineering and IT, University of Technology Sydney, P.O. Box 123, Broadway, Ultimo, NSW 2007, Australia

[b] School of Chemical Engineering, Chonnam National University, 77 Yongbong-ro, Gwangju 61186, Republic of Korea

*Corresponding author; Email: Saravanamuth.Vigneswaran@uts.edu.au

Abstract

Selective copper (Cu) recovery from wastewater mitigates environmental pollution and is economically valuable. Mesoporous silica adsorbents with manganese loading and amine-grafting, SBA-15-NH_2 and Mn-SBA-15-NH_2, were synthesized. The characteristics of the synthesized adsorbents were evaluated in detail in terms of its crystal structure peaks, surface area and pore size distribution, transmission electron microscope and X-ray photoelectron spectroscopy. The results established the high selective Cu adsorption capacity of Mn-SBA-15-NH_2 in a mixed heavy metal solution, maintaining 96% competitive adsorption as that of a single Cu solution. Comparatively, Cu adsorption on SBA-15-NH_2 decreased by half due to high competition with other heavy metals. Optimal Cu adsorption occurred at pH 5. This pH condition enabled grafted amine group in Mn-SBA-15-NH_2 to form strong chelating bonds with Cu, avoiding protonation of amine group (below pH 5) as well as precipitation (above pH 5). The adsorption equilibrium well fitted to Langmuir and Freundlich isotherm models, while kinetic results were represented by models of linear driving force approximation (LDFA) and pore diffusion model (PDM). High regeneration and reuse capacity of Mn-SBA-

15-NH_2 were well established by its capacity to maintain 90% adsorption capacity in a multiple adsorption-desorption cycle. Cu was selectively extracted from Mn-SBA-15-NH_2 with an acid solution.

Keywords

Mesoporous silica; Amine-grafting; Manganese loading; Adsorption; Copper; Heavy metals

1. Introduction

The discharge of industrial and mining wastewater containing elevated concentration of heavy metal results in severe water contamination (Da'na and Sayari, 2012; Mureseanu et al., 2008; Naidu et al., 2019; Zhao et al., 2017). Heavy metals are not biodegradable, and therefore, tend to accumulate and remain in water bodies for a long time. This poses long term detrimental effect to ecosystem and human health. Amongst the heavy metals, copper (Cu) tends to be present in high concentrations in wastewater. This is because Cu is regularly used in various industrial applications, such as printed circuit boards, semiconductor devices, pipelines, and battery manufacturing (Cui and Zhang, 2008; Hadi et al., 2015; Lee et al., 2016; Niu and Li, 2007; Xue et al., 2012). Wastewater containing Cu must be treated prior to discharge as Cu is highly toxic, even if present in trace concentration (Nagajyoti et al., 2010). At the same time, Cu is an economically valuable metal (Glöser et al., 2015) given its vast industrial application. Thus, removing and selectively recovering Cu from wastewater, will be both environmentally and economically beneficial.

Various remediation approaches are generally applied for heavy metal removal from wastewater such as chemical precipitation, ion exchange/adsorption, membrane filtration, and electrochemical methods (Fu and Wang, 2011). Adsorption is a promising approach due to its convenience, ease of operation and cost effectiveness (Cai et al., 2019; Da'na and Sayari, 2012). More importantly, adsorption possess the capacity to selectively recover valuable metals such as Cu from wastewater containing mixed constituent of heavy metals. Conventionally, absorbents such as zeolite (Ryu et al., 2019), pumice (Yavuz et al., 2008), activated carbon (Anirudhan and Sreekumari, 2011), and chitosan (Feng et al., 2019; Xiao et al., 2019) are used for removal of heavy metals from wastewater. However, these adsorbents

exhibit low heavy metal adsorption capability for practical application and do not possess selective adsorption capacity in mixed solutions. One potential method to enhance heavy metal removal efficiency is by increasing the surface area of absorbents.

In this regard, mesoporous silica is a promising material that possess large surface area. This apart, mesoporous silica exhibit several other advantageous features such as high thermal and physical stabilities, tuneable and uniform porosity and flexibility towards surface chemical modification (McManamon et al., 2012; Szegedi et al., 2011). In particular, mesoporous materials of SBA series consist of thick pore walls, large and tuneable pore size (2 – 30 nm) (Anbia et al., 2010). The triblock copolymer surfactant acts as a structure-directing agent (SDA) for SBA-15 preparation (Kim et al., 2014). However, in spite of the various beneficial features of SBA-15, in its natural condition, it cannot selectively adsorb contaminants such as heavy metals from wastewater as it lacks active sites and attractive functional groups for ions (Jiang et al., 2007; Liang et al., 2017).

Thus, chemical functionalization of SBA-15 is necessary to produce active sites for adsorption and enhance selective removal of heavy metals. A number of different SBA-15 modification methods have been explored (Ezzeddine et al., 2015; Hernández-Morales et al., 2012; Jiang et al., 2007; Liang et al., 2017). For instance, Saad et al. (2007) synthesized and modified SBA-15 using an amino-group source of (3-aminopropyl) triethoxysilane (APTES) with two different modification methods, co-condensation and post synthesis (Saad et al., 2007). Amine grafted SBA-15 enabled to achieve high heavy metal removal because amino-propyl moieties reacts with silanol groups on the surface (Benhamou et al., 2013; Da'na et al., 2011; Yokoi et al., 2006). In another study, Lei et al (2015) carried out a combined modification of manganese loading and amine-grafted SBA-15 for heavy metal adsorption. Amine grafting on SBA-15 with manganese loading enabled to achieve high selective Cu

extraction in a competitive adsorption study (Lei et al., 2015). The mechanism of manganese modification with amine on SBA-15 has been evaluated in detail for applications such as catalyst (Saikia and Srinivas, 2009; Saikia et al., 2007). However, there is still limited research with regards to the mechanism of manganese modified SBA-15 with amine for heavy metal adsorption. Further, theoretical analysis based on isotherm parameters such as surface and pore diffusion models and selective capacity of Cu in a mixed heavy metal solution has not been explored in detail.

In this study, the role of manganese loading and grafted amine-groups on SBA-15 towards selective Cu removal is investigated in detail. For this reason, SBA-15 synthesis was carried out in a batch hydrothermal reaction and modified by manganese loading and amine-grafting. The characteristics and adsorption capacity of the modified SBA-15 for heavy metal (Cu, Zn, Ni and Mn) removal were evaluated in detail. Experimental data were fitted to equilibrium models such as Langmuir and Freundlich and kinetic models such as linear driving force approximation and pore diffusion models. Further, regeneration and reusability of the adsorbents were also evaluated to establish the cost effectiveness and practical applicability of the adsorbents.

2. Material and methods

2.1. Materials

Tetraethyl orthosilicate (TEOS) (98%, Sigma-Aldrich) and poly(ethylene glycol)-block-poly(propylene glycol)-block-poly(ethylene glycol) (P123) were used as a silica precursor and a structure direct agent (SDA), respectively. 2 M of hydrochloric acid (HCl) was prepared by using 34% HCl solution purchased from Sigma-Aldrich to hydrolyze the silica precursor, TEOS, for self-assembly reaction onto the SDA, P123. $KMnO_4$ (Sigma-Aldrich)

was used for manganese modification. (3-aminopropyl) triethoxysilane (APTES, Sigma-Aldrich) and toluene were used for amine-grafting onto the mesoporous silica material, SBA-15. $CuSO_4$, $ZnSO_4$, $MnSO_4$ and $NiNO_3$ were used to prepare heavy metal solutions for batch adsorption experiments. 0.01 M of sodium hydroxide (NaOH) (>98%, Sigma-Aldrich) and HCl solutions were used for pH adjustment. 0.01 M HCl solution was used in desorption experiments.

2.2. Preparation of adsorbent

SBA-15 was synthesized via a hydrothermal reaction based on a previously reported method (Zucchetto et al., 2018). 12 g of P123 was added in a mixture of 90 ml of Milli-Q water and 480 ml of 2 M HCl at a room temperature (24 ± 1 ºC). 25.5 g TEOS was then added slowly into the mixture for the hydrolysis by acidic condition (Wei et al., 2006). Thereafter, the mixture was kept at 35 ºC for 20 h and 100 ºC for 24 h in a polypropylene bottle for hydrothermal reaction. The precipitated powder was then dried at 70 ºC in an oven after filtration and washed with Milli-Q water. It was then calcined at 550 ºC for 3 h in an air condition to get rid of the surfactant, P123, from the ordered structure with silica sources.

2.3. Modifications of adsorbent

2.3.1. Manganese loading

Modification of SBA-15 with manganese loading was carried out by adding 1 g of the prepared SBA-15 into 200 ml of 0.1 M $KMnO_4$ aqueous solution (Lei et al., 2015). The mixture of SBA-15 and $KMnO_4$ was mixed for 3 h at ambient temperature. The resultant solid powder was filtered and washed with Milli-Q water thoroughly and thereafter oven dried at 70 °C, to produce manganese doped mesoporous silica, Mn-SBA-15.

128

129 2.3.2. Amine-grafting

130 Surface modification of mesoporous silica material by amine-groups was carried out using
131 post-grafting method based on a previously reported method (Da'na and Sayari, 2011; Saad
132 et al., 2007). 1.0 g of prepared SBA-15 and Mn-SBA-15 were dispersed into 100 ml of dry
133 toluene. Thereafter, 1 ml of APTES was added. The solution was refluxed for 10 h at 110 ºC
134 to enable reaction to occur between OH groups of mesoporous silica's surface and amino-
135 propyl groups of the APTES. The final products SBA-15-NH_2 and Mn-SBA-15-NH_2 were
136 filtered, washed thoroughly with ethanol and oven-dried at 70 ºC.

137

138 2.4. Absorbent characterizations

139 2.4.1. Crystal structure

140 Powder X-ray diffraction (XRD) analysis was used to determine the structure of the
141 adsorbents prepared. XRD analysis was carried out with a X-ray diffractometer with high
142 resolution (X'Pert PRO Multi-Purpose X-Ray Diffractometer) operated with the radiation
143 source of Cu-Kα. The system was operated at room temperature in 2 theta range of 0 to 10 º
144 with a 2º/min scan rate at 20 mA and 40 kV.

145

146 2.4.2. Surface area and pore size distribution

147 The physical properties (surface area and pore size distribution) of the prepared adsorbents
148 were determined after performing nitrogen adsorption/ desorption isotherm experiments.
149 They were measured at 77 K (Nanoporosity, Mirae SI Korea). The mesopore volume and the
150 pore size distribution were estimated by Barrett-Joyner-Halenda (BJH) method, while surface
151 areas of the samples were obtained from the Brunauer-Emmett-Teller (BET) method.

152

153 2.4.3. Surface morphology and element contents

154 The surface morphologies of adsorbents were investigated using a field emission
155 transmission electron microscope (FETEM, JEM-2100F) at 200 kV and the element contents
156 of all samples were identified by X-ray photoelectron spectroscopy (XPS) using Kα radiation
157 with seven Channeltron detectors. Fourier transform infrared spectroscopy (FTIR)
158 spectrometer (FTIR-410, Jasco Co.) was used to obtain for investigating the chemical bonds
159 and vibrations.

160

161 2.5. Influence of pH

162 pH effect on heavy metal adsorption was investigated using solutions of different pH (1 to 5).
163 They were prepared with 0.1 M NaOH and HCl aqueous solutions. 0.01 g of the prepared
164 adsorbent was suspended in beakers containing 50 ml of Cu solution (300 mg/L) with varied
165 initial pH. The flasks were agitated at 120 rpm for 24 h in a flat shaker at ambient
166 temperature (24 ± 1 °C).

167

168 2.6. Adsorption study

169 2.6.1. Equilibrium

170 Batch equilibrium adsorption of heavy metals (Cu, Zn, Ni and Mn) on the prepared pristine,
171 manganese-doped, and amine-grafted adsorbents was carried out. 0.01 g of each adsorbents
172 and 50 ml of heavy metal solution were mixed into beakers. The beakers were placed in a flat
173 shaker at room temperature (24 ± 1 ºC) for a day to reach equilibrium. The preliminary
174 experiment showed that a period of 24 h was sufficient to reach equilibrium. Single-
175 component adsorption experiments were conducted with 10 – 300 mg/L of initial

concentrations of heavy metals, while 10 to 100 mg/L of metals were used for multi-component adsorption experiment. These concentrations selected were based on the presence of heavy metals in wastewater (Jalali and Moradi, 2013; Özdemir et al., 2009; Šćiban et al., 2007; Singh and Agrawal, 2007). Microwave Plasma-Atomic Emission Spectrometer (MP-AES, MP-AES-4100 Agilent) was used to determine the heavy metal concentrations in treated solutions. The equilibrium adsorption capacity, Q_e (mmol/g), was determined using Eq. (1):

$$Q_e = V(C_i - C_e)/M \quad (1)$$

where, V is the solution volume (L) and M is sorbent mass (g). C_i and C_e are the concentrations (mg/L) of the heavy metals at initial and equilibrium, respectively.

Langmuir and Freundlich isotherm models were employed to obtain equilibrium adsorption data:

Langmuir isotherm: $Q_e = Q_m b C_e/(1 + bC_e)$ (2)

Freundlich isotherm: $Q_e = K_F {C_e}^{1/n}$ (3)

where, Q_m and b are the maximum sorption capacity (mmol/g) and Langmuir constant (L/mmol) related to the affinity of the binding sites, respectively. Freundlich constant is related to sorption affinity, K_F (g^{1-n} $L^n g^{-1}$) and 1/dimension less parameter (1/n) was related to surface heterogeneity (Ali et al., 2016; Foo and Hameed, 2010; Gonzales et al., 2016) were also used in adsorption modeling.

200

201 2.6.2. Kinetics

202 The kinetic adsorption experiments were carried out in batch systems. Each beaker contained
203 0.01 g adsorbent and 50 ml of 50 mg/L Cu solution. The beaker with the solution was
204 agitated at room temperature (24 ± 1 ºC) and samples were collected at different time
205 intervals until 24 h for metal analysis. In this study, the adsorption data were analyzed by
206 linear driving force approximation (LDFA) model due to its simplicity and feasibility in
207 describing adsorption of Cu ions from aqueous solution on modified SBA-15 samples (Kim
208 et al., 2008). The mass transfer rate between solid and liquid phases can be described by the
209 LDFA model as:

210

211 $$d\bar{Q}/dt = 3k_f(C_b - C_s)/R_p\rho_p = k_s(Q_s - \bar{Q}) \quad (4)$$

212

213 where

214

215 $$k_s = 15D_s/{R_p}^2 \quad (5)$$

216

217 where k_s is the mass transfer coefficient of solid side (1/s), k_f is the film mass transfer
218 coefficient (m/s), R_p is the radius of adsorbent particle (m), C_b is bulk concentration (mg/L),
219 C_s is equilibrium concentration (mg/L), $\bar{Q}$ is the average value of adsorbed particle amounts,
220 t is the time passed in a batch reactor, Q_s is the concentration of adsorbed phase at the
221 external surface of adsorbent particle (mmol/g), ρ_p is the particle density (kg/m^3), and D_s is
222 effective surface diffusion coefficient (m^2/s).

223 Adsorption occurs both through external film and internal pore (Hariharan et al., 2012). Thus,

the kinetic data were also determined by pore diffusion model (PDM) using the following equations:

$$\varepsilon_p(\partial C_p/\partial t) + \rho_p(\partial Q/\partial t) = D_p[(\partial^2 C_p/\partial r^2) + (\partial C_p/\partial r)/r] \quad (6)$$

Corresponding boundary conditions and initial concentration are:

$$\partial \mathrm{C}_p/\,\partial \mathrm{r} = k_f(C_b - C_p)/D_p\varepsilon_p \; at \; r = R_p \quad (7)$$

$$\mathrm{C}_p = C_0 \; at \; t = 0 \quad (8)$$

$$\partial \mathrm{C}/\,\partial \mathrm{r} = 0 \text{ at } \mathrm{r} = 0 \quad (9)$$

where ε_p is the particle porosity, C_p is the concentration of ions at the inside of particle (mg/L), D_p is the effective pore diffusion coefficient (m^2/s), and r is the radial distance (m).

2.7. Metal desorption and adsorbent regeneration

Reusability of the manganese doped and/or amine-grafted SBA-15 was tested with 10-time adsorption and desorption recycle experiments. After each adsorption experiments, spent adsorbents were recovered by filtration from the working solution. For the desorption step, the recovered powder was treated by 0.01 M HCl solution for Cu recovery (Da'na and Sayari, 2011). Acidic solution can bring about heavy metal desorption through protonation (NH_3^+) of the grafted amine groups (NH_2). The recovered adsorbents were dried at 80 ºC after filtration and washing with Milli-Q water. Prior to the use, the dried white powder has to be neutralized. Therefore, the powder was stirred in a solution of 0.01 M NaOH for 1 h. For the further adsorption experiments, the regenerated silica powder was used with another heavy metal

248 solution.

249

250 3. Results and discussion

251 3.1. Adsorbent characterization

252 3.1.1. Crystal structure

253 X-ray diffraction pattern by XRD analysis revealed that the crystal structure pattern of
254 adsorbents SBA-15, Mn-SBA-15, SBA-15-NH_2 and Mn-SBA-15-NH_2 contained three peaks
255 in the low 2 theta range of 0 – 10º (Fig. 1). Previous studies have established the crystal
256 structure of a virgin SBA-15 contain one high peak (1 0 0), and two tiny peaks of (1 1 0) and
257 (2 0 0) (Kim et al., 2015). The XRD results implies that the prepared SBA-15 in this work
258 was synthesized well with highly ordered hexagonal structured material. The three crystal
259 peaks were still maintained even after Mn modification on the virgin SBA-15. This indicates
260 that the 2-dimensional (2D) hexagonal structure of SBA-15 was stable during Mn loading
261 (Lei et al., 2015). All the three adsorbents showed closely similar intensity of the main peak
262 (1 0 0), indicating that hexagonal structures of SBA-15 was not collapsed after the
263 modification processes (Ryu et al., 2018). However, 2 peaks of (1 1 0) and (2 0 0)
264 significantly decreased after amine-grafting on SBA-15 and Mn-SBA-15. Other studies
265 (Aguado et al., 2009; Calleja et al., 2011; Chang et al., 2009) also showed the decrease in
266 minor peaks of SBA-15-NH_2 (Shahbazi et al., 2011). The decrease is associated to pore
267 blocking by amine (–NH_2) groups bonded on the surface of SBA-15.

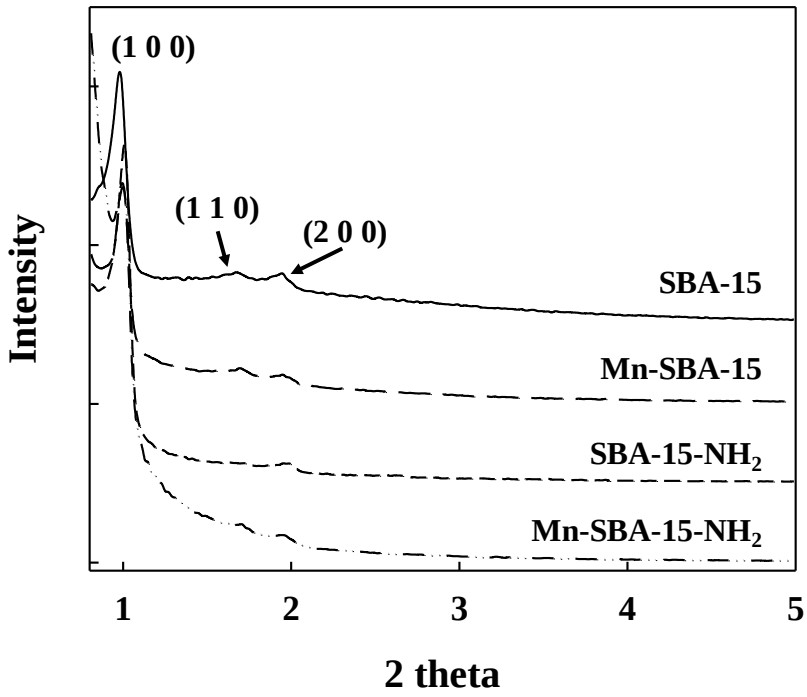

Fig. 1. The XRD patterns of SBA-15, Mn-SBA-15, SBA-15-NH_2 and Mn-SBA-15-NH_2

3.1.2. Chemical properties

Fig. 2. Presents FT-IR spectra of the SBA-15, Mn-SBA-15, SBA-15-NH_2 and MN-SBA-15-NH_2. Typically, SBA-15 consists of Si-O-Si bands that appear around 1080 and 800 cm^{-1} and hydroxyl group (-OH) attributed to silica network shown at around 960 cm^{-1} (Wang et al., 2015). After Mn modification, a decrease in the vibration band for Si-OH at 970 cm^{-1} was observed. This implies the successful reaction between Si-OH and Mn (Li et al., 2007). Additional spectra at around 2900 and 1500 cm^{-1} were observed on the modified SBA-15-NH_2 and Mn-SBA-15-NH_2. They are attributed to N-H vibration band by amine-grafting on SBA-15 (Szegedi et al., 2011; Yan et al., 2011). The FT-IR spectra enabled to confirm whereas the modifications of SBA-15 were successfully carried out or not.

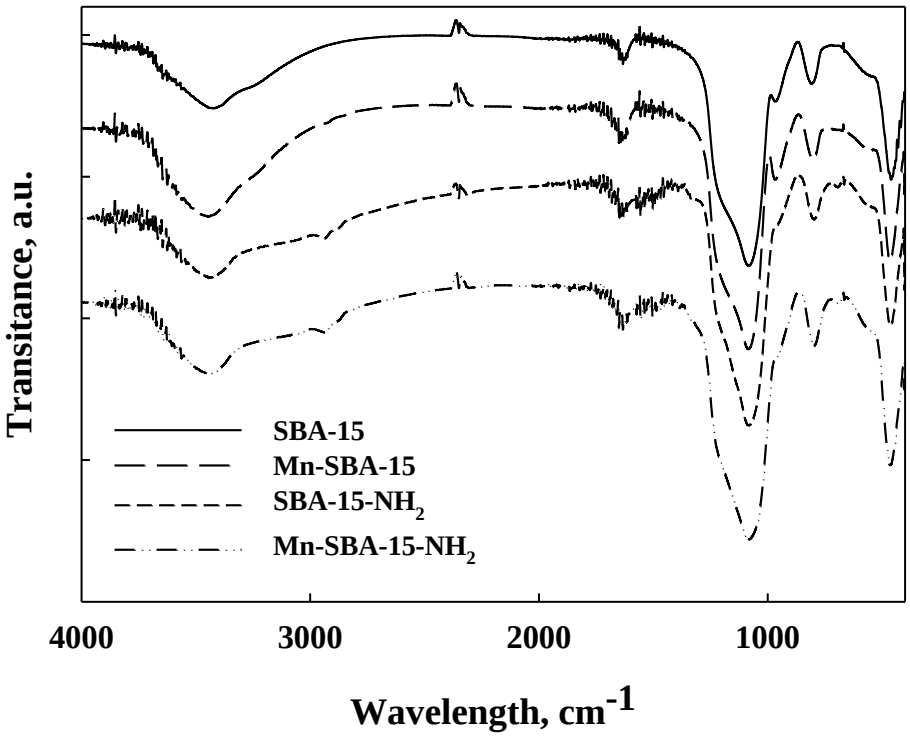

281

282 Fig. 2. FT-IR spectra of prepared SBA adsorbents

283

284 3.1.3. Surface area and pore size distribution

285 The physical properties (surface area and pore size distribution) of the adsorbents are
286 summarized in Table 1. The adsorption and desorption isotherm of nitrogen at 77 K on
287 adsorbents (Fig. S1), show that all graphs exhibit type IV adsorption based on the BDDT
288 classification. This is in line with the results on mesoporous materials (Lombardo et al.,
289 2012). The specific surface area of virgin SBA-15 measured by BET method was 830 m^2/g
290 for the virgin SBA-15. The BET surface area of Mn-SBA-15, SBA-15-NH_2 and Mn-SBA-15-
291 NH_2 decreased to 700, 310 and 310 m^2/g due to pore blocking by chemical bonding of SBA-
292 15 with Mn and amine functional groups. These results can be explained by the porosity of
293 adsorbents. The pore size distributions of samples are shown in Fig. S2. The peak position

shifted from around 6 nm to 5 nm after amine-grafting on SBA-15. On the other hand, an additional minor peak was visible at around 4 nm with Mn modified adsorbents (Mn-SBA-15 and Mn-SBA-15-NH_2). It implies that some portion of pores were blocked by Mn application which caused in decrease of the pore size. Total pore volume of virgin SBA-15 was 1.24 cm^3/g and it decreased to 1.11, 0.73, and 0.76 cm^3/g for Mn-SBA-15, SBA-15-NH_2, and Mn-SBA-15-NH_2, respectively. Likewise, mean pore diameter of SBA-15 and Mn-SBA-15 reduced from 4.6 and 4.5 to 4.0 nm after amine grafting. Overall, the physical properties of the adsorbents demonstrate the success in modification of SBA-15.

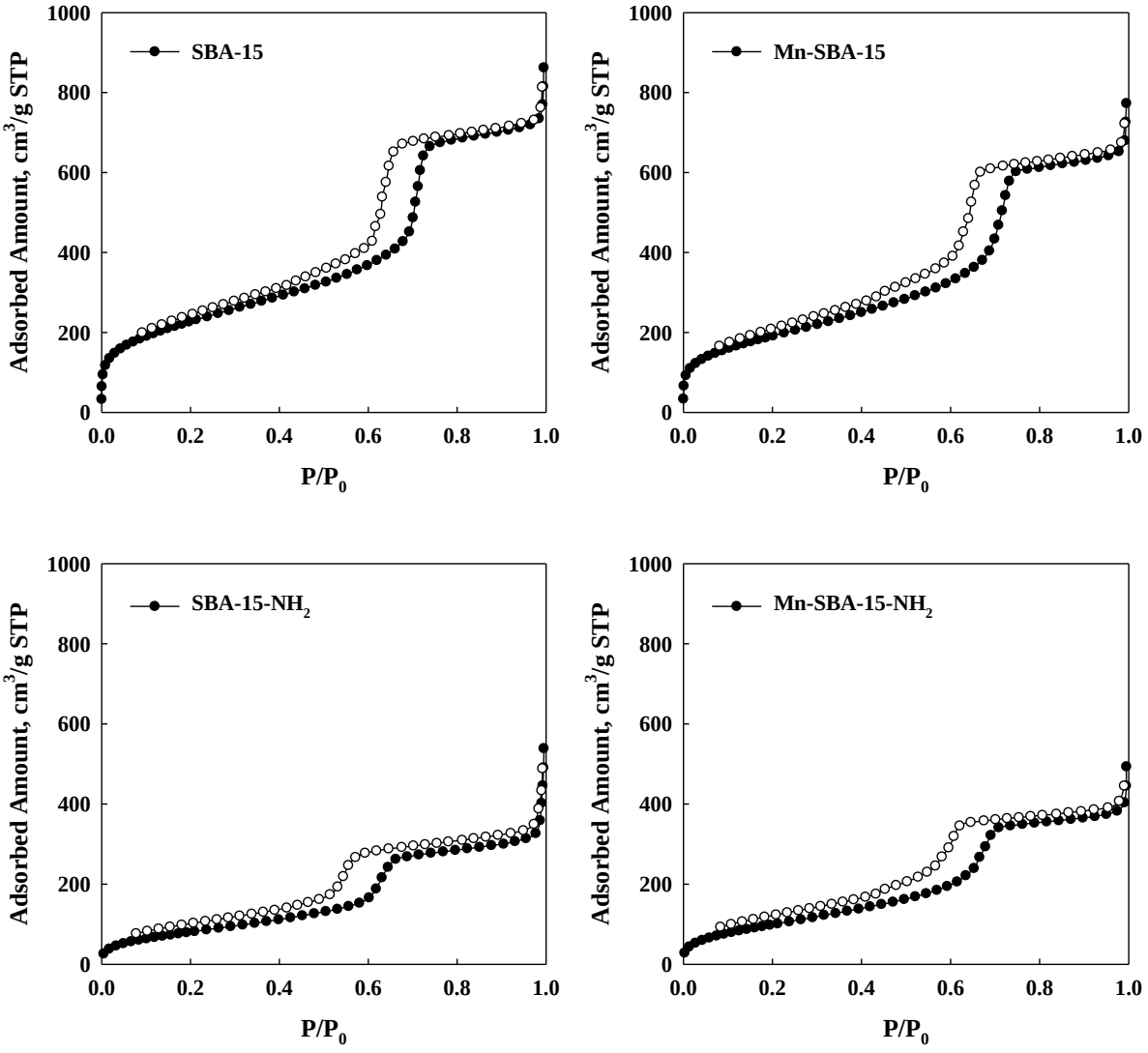

303 Fig. S1. Isotherms for nitrogen adsorption and desorption of prepared samples

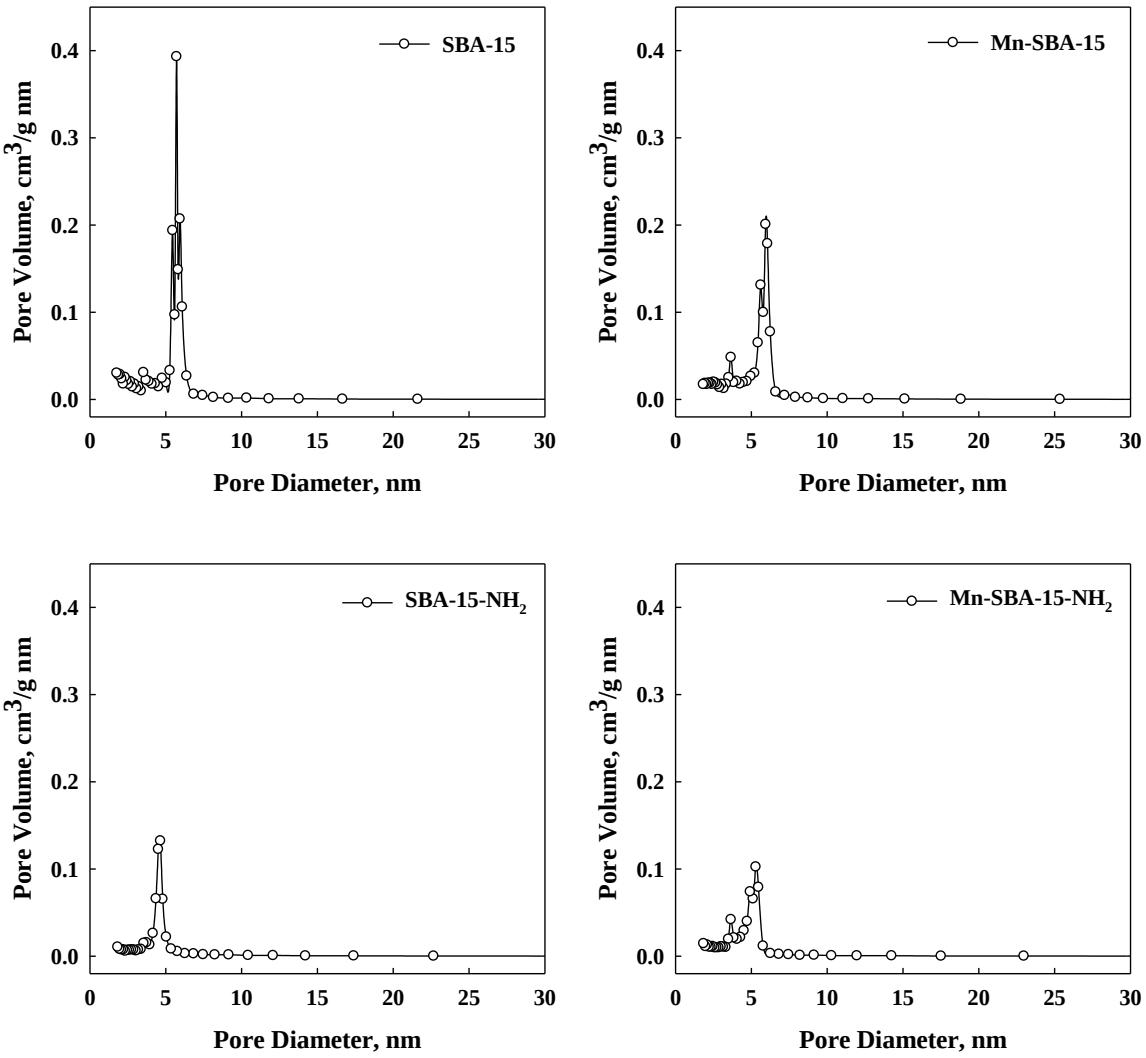

304

305 Fig. S2. Adsorbent BJH pore size distribution profiles

306

307 Table 1. Adsorbent physical properties

Adsorbents	BET surface area m^2/g	Total pore volume cm^3/g	Mean pore diameter nm
SBA-15	830	1.24	4.6
Mn-SBA-15	700	1.11	4.5
SBA-15-NH_2	310	0.73	4.0

Mn-SBA-15-NH_2	310	0.76	4.0

308

309 3.1.4. Surface morphology and element content

310 TEM images of the virgin and modified SBA-15 adsorbents (Fig. 3) exhibit the well-ordered
311 and 2D hexagonal structured array of the mesoporous material. The surface morphology
312 indicated that the modified adsorbents were able to maintain well-ordered structure as that of
313 the virgin SBA-15. The XPS spectra revealed element contents of Si, O, N and Mn of the
314 adsorbents (Fig. 4). In particular, high resolution XPS curves of O 1s and Si 2p in the region
315 of 530 – 535 eV and 103 – 110 eV were attributed to Si-O-Si bonds (Table 2). The presence
316 of N 1s peaks in the range of 400 – 405 eV on SBA-15-NH_2 and Mn-SBA-15-NH_2 indicated
317 the presence of NH_2 upon amine grafting (Gao et al., 2007). Further, minor peaks around 645
318 eV were observed on Mn-SBA-15-NH_2 and this was attributed to Mn loading into the pore of
319 SBA-15.

320

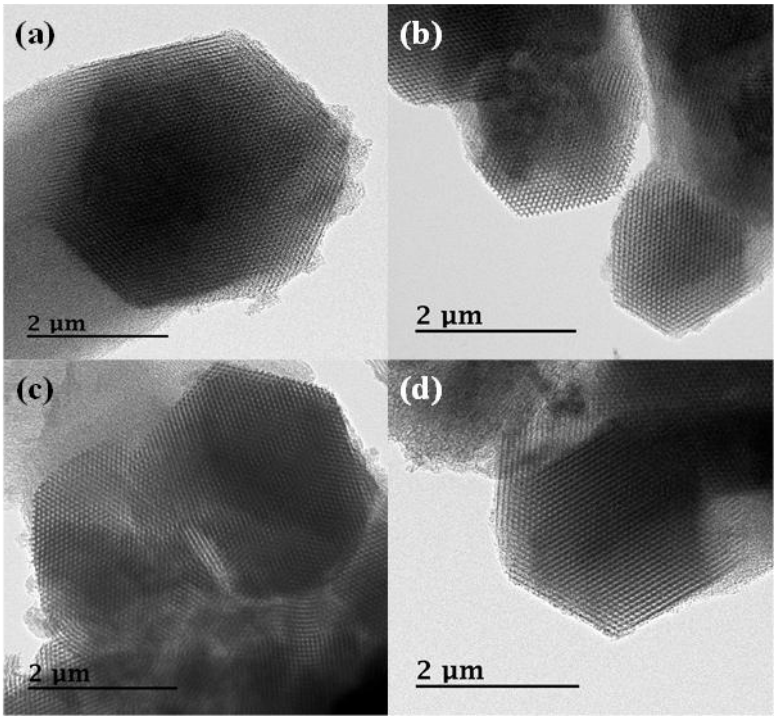

321

322 Fig. 3. TEM images of adsorbents (a) SBA-15, (b) Mn-SBA-15, (c) SBA-15-NH_2 and (d)

323 Mn-SBA-15-NH_2

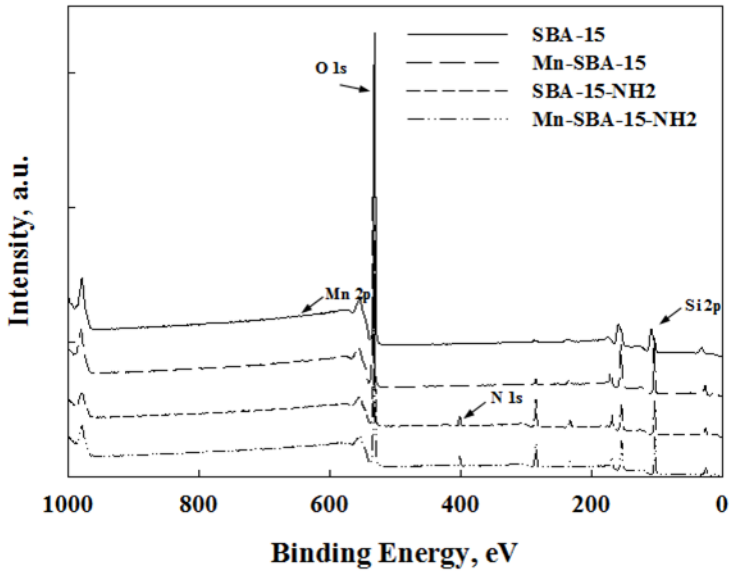

324

325 Fig. 4. XPS spectra of virgin and modified SBA-15

326

327 Table 2. XPS binding energy (eV) of virgin and modified SBA-15

Adsorbents	Si 2p	O 1s	N 1s	Mn 2p
SBA-15	108.6	531.9	-	-
Mn-SBA-15	104.1	533.2	-	646.4
SBA-15-NH_2	103.3	532.3	401.76	-
Mn-SBA-15-NH_2	103.2	532.2	401.33	645.1

328

329 3.1.5. Influence of pH

330 Cu adsorption by SBA-15-NH_2 was highly influenced by pH of the solution (Fig. 5). Minimal

331 Cu adsorption (close to zero) occurred at pH of 1 – 2. This was due to protonation of amine

332 groups, $–NH_2$ to $–NH_3$ (Da'na and Sayari, 2011). A trend of higher Cu adsorption capacity

333 was observed as the solution pH was increased above 2. A maximum Cu adsorption was

achieved at pH 5. The mechanisms describing the influence of pH towards Cu adsorption by amine grafted SBA-15 is depicted in Fig. 6 (Da'na and Sayari, 2011). The grafted amine groups (NH_2) on SBA-15 easily form complexes with Cu ions at pH above 4. However, the protonated amine groups, $–NH_3^+$, do not form bonds with Cu ions easily when the pH value is below 4. Meanwhile, above pH 5, a tendency of copper precipitation occurs. Hence all heavy metal equilibrium experiments were carried out at optimum pH 5.

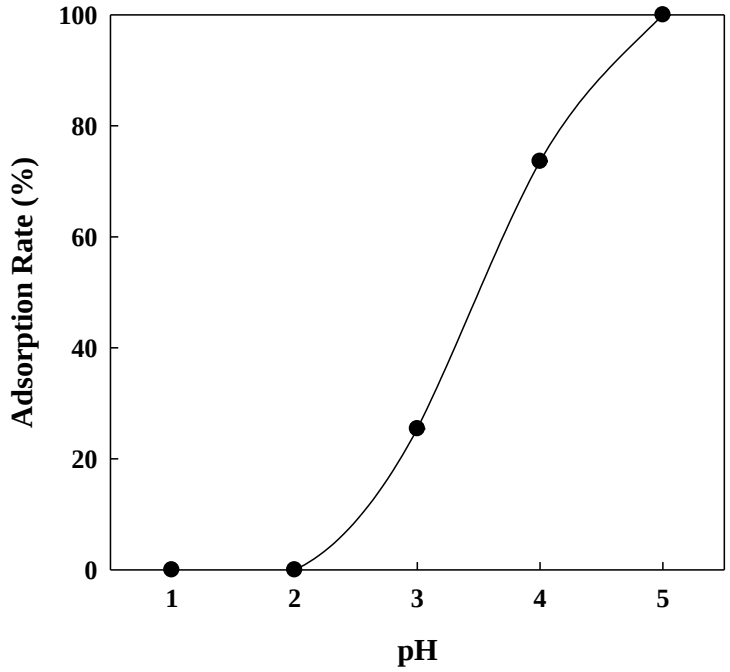

Fig. 5. Adsorption rate of Cu on SBA-15-NH_2 as a function of solution pH (experimental conditions: adsorbent dose: 0.2 g/L, Cu concentration: 300 mg/L, equilibrium time: 24 h)

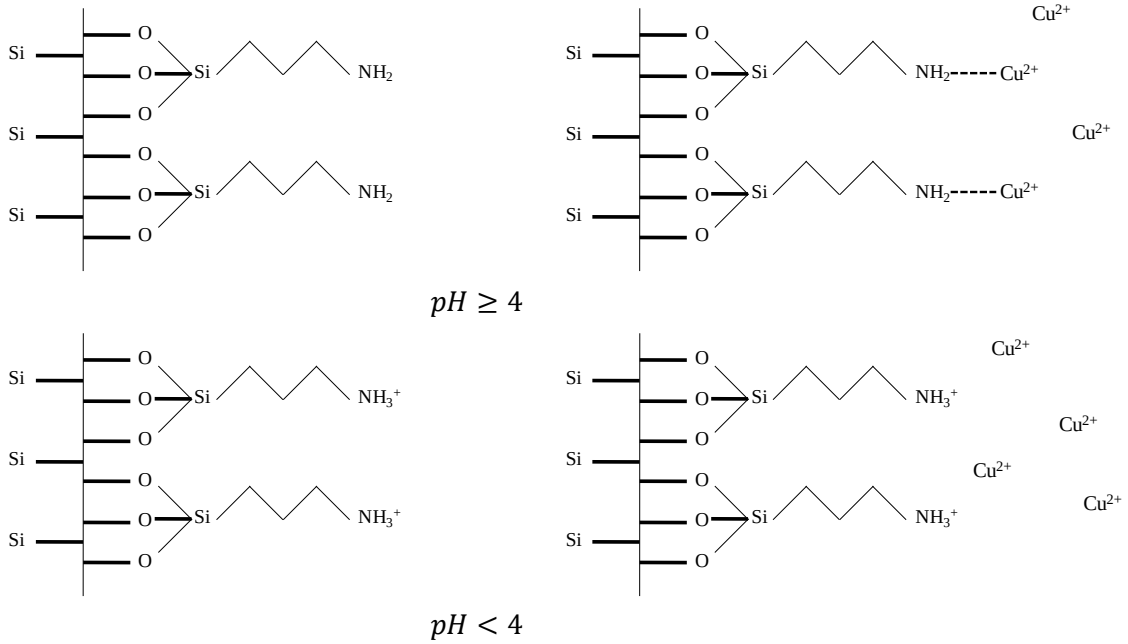

Fig. 6. Depiction of Cu adsorption mechanisms on the amine-grafted SBA-15

3.2. Adsorption study

3.2.1. Equilibrium

3.2.1.1. Single component adsorption

Fig. 7 shows the adsorption isotherms at room temperature (24 ± 1 °C) for individual heavy metals (Cu, Zn, Ni and Mn) on prepared adsorbents (SBA-15, SBA-15-NH_2, and Mn-SBA-15-NH_2) at pH 5. All data were satisfactorily fitted with both Langmuir and Freundlich equations according to R^2 values (Table 3). The Langmuir model describes monolayer adsorption, thus Freundlich isotherm is the practical model on adsorption with heterogeneous surface (Popuri et al., 2009; Shahbazi et al., 2011). The heavy metal adsorption capacity by SBA-15 was minimal (0.14 – 0.50 mmol/g). Comparatively, the adsorption capacity of heavy metals by SBA-15-NH_2 were 4 – 9 times higher. Specifically, adsorption capacity of Cu, Zn, Ni and Mn were 1.86, 1.26, 1.28 and 1.14 mmol/g with SBA-15-NH_2. Meanwhile, Mn-SBA-15-NH_2 showed improved adsorption capacities of heavy metals than SBA-15-NH_2 (12 – 43%

higher). Specifically, adsorption capacity of Cu, Zn, Ni and Mn were 2.08, 1.44, 1.84 and 1.28 mmol/g with Mn-SBA-15-NH_2. The amine group grafted on the modified adsorbent is a major factor that enhances adsorption capacity of heavy metals compared to virgin SBA-15 (Aguado et al., 2009). Further, in the case of Mn-SBA-15-NH_2, a large portion of amine groups is able to be grafted on Mn-SBA-15. This is because manganese oxide reacts well with amine (Zhao et al., 2015; Zhu and He, 2012). Thus, Mn-SBA-15-NH_2 was able to achieve higher heavy metal adsorption capacity compared to SBA-15-NH_2.

In individual single metal solutions, the heavy metal adsorption capacity with SBA-15, SBA-15-NH_2 and Mn-SBA-15-NH_2 followed the order of Cu>Ni>Zn>Mn. Likewise, a previous study (Da'na and Sayari, 2012; Mureseanu et al., 2008; Sreenu et al., 2016) showed higher Cu adsorption compared to other heavy metals such as Ni and Zn when mesoporous silica material with amine grafting was used.

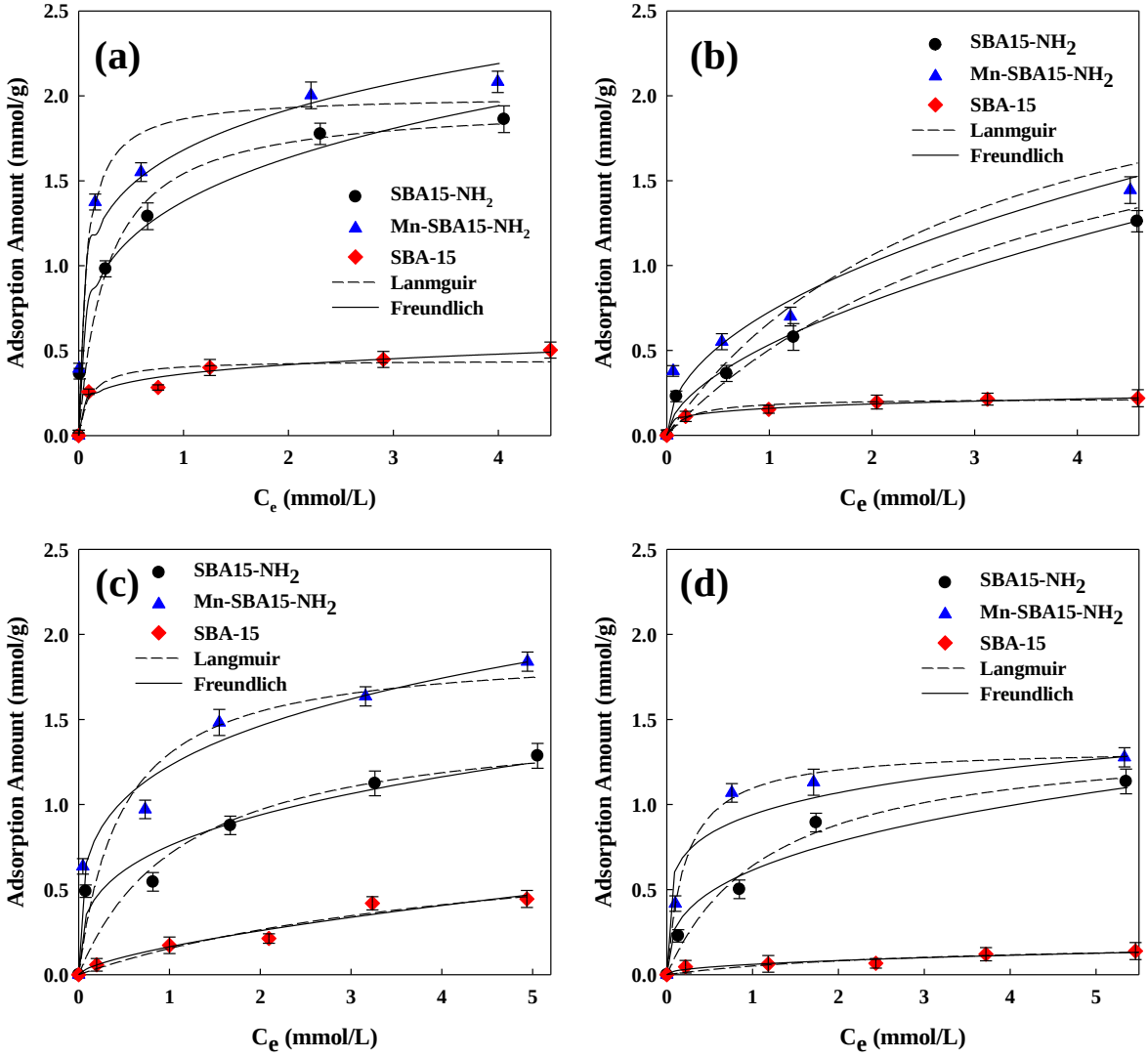

374
375

376 Fig. 7. Adsorption isotherm graphs on synthesized adsorbents for (a) Cu, (b) Zn, (c) Ni and (d)

377 Mn (experimental conditions: 0.2 g/L adsorbent dose, pH=5, equilibrium time: 24 h)

Table 3. Isotherm parameters for heavy metal adsorption on prepared adsorbents

Equation	Parameter	Sample											
		Cu adsorption			Zn adsorption			Ni adsorption			Mn adsorption		
		SBA-15	SBA-15-NH_2	Mn-SBA-15-NH_2	SBA-15	SBA-15-NH_2	Mn-SBA-15-NH_2	SBA-15	SBA-15-NH_2	Mn-SBA-15-NH_2	SBA-15	SBA-15-NH_2	Mn-SBA-15-NH_2
Langmuir	q_m	0.44	1.96	2.00	0.22	2.49	2.65	0.92	1.53	1.91	0.20	1.42	1.33
	b	9.99	3.70	13.55	4.64	0.25	0.33	0.20	0.86	2.12	0.34	0.82	4.60
	R^2	0.99	0.99	0.98	0.94	0.99	0.98	0.97	0.99	0.99	0.91	0.99	0.99
Freundlich	K_F	10.03	31.40	48.39	4.26	3.29	6.21	0.66	12.66	25.72	0.54	8.41	24.64
	n	4.98	4.05	5.24	4.68	1.77	2.05	1.52	3.24	3.95	2.21	2.88	5.41
	R^2	0.99	0.99	0.97	0.99	0.99	0.99	0.96	0.99	0.99	0.92	0.97	0.92

379 3.2.1.2. Multi components adsorption

380 The effect of metal competition and selective Cu extraction was also evaluated in a multi
381 component solution containing heavy metals (Cu, Zn, Ni and Mn) mixed in equal
382 concentration ranging from 10 mg/L to 100 mg/L.

383 Adsorption capacity for competitive heavy metal removal in terms of equilibrium
384 concentration (Fig. 8) showed that the adsorption capacity for Cu on SBA-15-NH_2 (1.01
385 mmol/g) decreased by 54% compared to that of single-component adsorption experiment (Fig.
386 7). This is attributed to competition with other heavy metals (Zn, Ni and Mn). On the other
387 hand, Mn-SBA-15-NH_2 was able to maintain 96% of adsorption capacity for Cu (2.01
388 mmol/g). The adsorption selectivity cannot be determined by single component adsorption
389 capacities for those metal ions (Koong et al., 2013).

390 Generally, the capacity of an adsorbent to maintain high selective ion extraction in a mixed
391 solution is associated to ion characteristics such as ion radius, absolute hardness and absolute
392 electronegativity. In this regard, the ion radius of Cu (0.71 Å), Zn (0.74 Å), Ni (0.69 Å) and
393 Mn (0.80 Å) (Table 4) do not exhibit significant difference, suggesting that ion radius does
394 not play a role towards the selective Cu adsorption capacity exhibited by Mn-SBA-15-NH_2.
395 Likewise, the absolute electronegativity is also similar for Cu^{2+} and Zn^{2+} (28.6 and 28.8) with
396 amine groups (Liu et al., 2008). However, the absolute hardness of Zn (10.8) is higher than
397 that of Cu (8.3). Theoretically, this implies that Mn-SBA-15-NH_2 should have a high
398 adsorption affinity for Zn compared to Cu, because amine is regarded as a harder donor atom
399 (Lee et al., 2016; Yu et al., 2007). Hence, the high selective Cu adsorption exhibited by Mn-
400 SBA-15-NH_2 in mixed metal solution is not entirely related to ion characteristics.

401

Table 4. Element characteristics

Metals	Ion radiuses (Å)	Absolute hardness	Absolute electronegativity
Cu	0.71	8.3	28.6
Zn	0.74	10.8	28.8
Ni	0.69	8.5	26.7
Mn	0.80	9.3	24.4

The affinity of high Cu selectivity by Mn-SBA-15-NH_2 could be related to chelating effect. This is because chemical groups such as amine, amide and aldehyde have different chelating ability with heavy metals. The amine group is regarded as a chemical group that can chelate well with Cu (Koong et al., 2013). Thus, it can be deducted that presence of amine groups on SBA-15 enables to form strong complexation with heavy metals, especially for Cu. Specifically, the manganese loaded and amine-grafted SBA-15 (Mn-SBA-15-NH_2) has an enhanced Cu selectivity than amine-grafted SBA-15 (SBA-15-NH_2) due to larger amount of grafted amine groups.

The adsorption capacity of the adsorbents used showed an increasing trend as the concentration of heavy metals was increased from 0 – 50 mg/L (Fig. 8). This is most likely due to the presence of higher amounts of other heavy metals (Zn, Ni and Mn) that reduced the adsorption of Cu. However, when the initial concentration of heavy metals was over 50 mg/L, only the adsorption of Cu increased, while the adsorption capacities for Zn, Ni and Mn did not increase any further. In fact, a decrease in absorption capacities of these heavy metals was observed. Similar trends have been reported in previous studies (Koong et al., 2013; Liu et al., 2008).

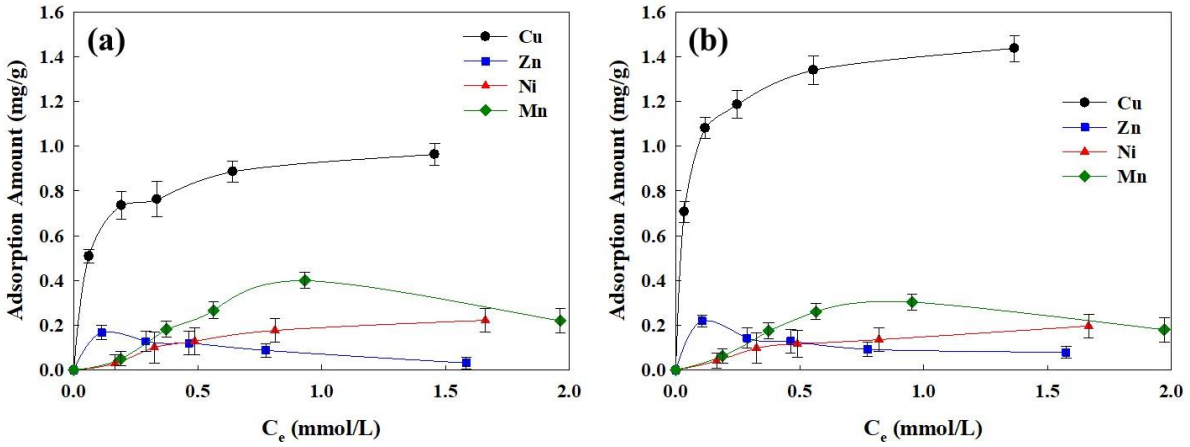

Fig. 8. Competitive adsorption of heavy metals on (a) SBA-15-NH_2 and (b) Mn-SBA-15-NH_2 (experimental conditions: 0.01 g of adsorbent dose in 50 ml of heavy metal solution at pH 5, equilibrium time: 24 h)

3.2.2. Adsorption kinetics

In this work, film mass transfer coefficient (k_f), surface diffusion coefficient (D_s), and pore diffusion coefficient (D_p) were estimated by LDFA and PDM models to represent the adsorption kinetics of SBA-15-NH_2 and Mn-SBA-15-NH_2 (Table 5). The kinetic adsorption phenomenon of the adsorbents was described using ordinary differential equations (ODEs) and polite dignified effective practical enthusiastic (PDEPE) in MATLAB program, numerically. Fig. 9 shows the good fitting of experimental values with theatrical values. All the kinetic coefficients (k_f, D_s and D_p) of SBA-15-NH_2 were observed to be higher than those of Mn-SBA-15-NH_2. This results indicated higher Cu adsorption rate on the surface of SBA-15-NH_2 compared to that of Mn-SBA-15-NH_2. The slower adsorption rate on Mn-SBA-15-NH_2 is attributed to the small pore size upon manganese modification. This was in line with the pore size evaluation described in Section 3.1.3 (Fig. S2, Table 1). Typically, the smaller

437 pore size of Mn-SBA-15-NH_2 compromised Cu diffusion rate but it increased the Cu
438 selective adsorption capacity.
439

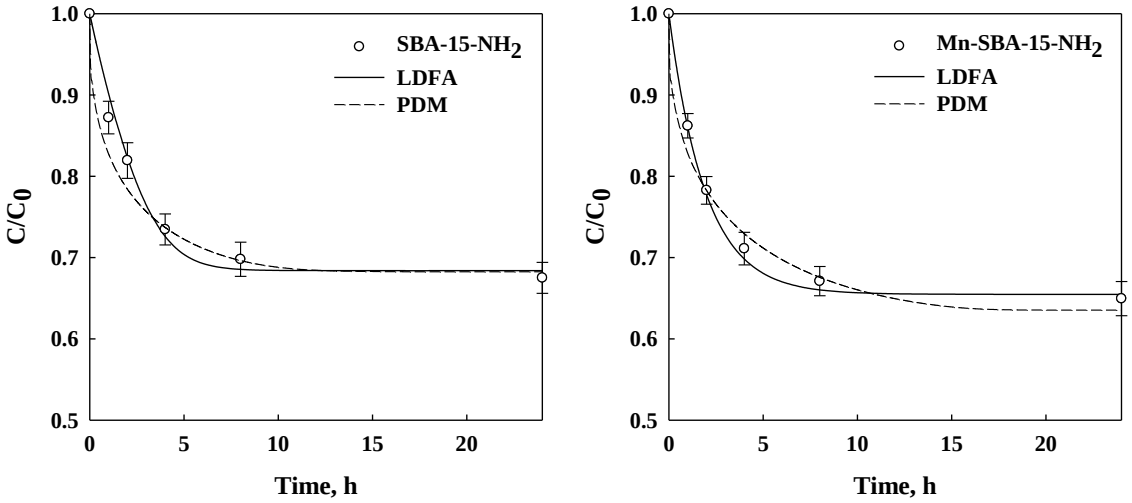

440

441 Fig. 9. Experimental adsorption kinetics of Cu on SBA-15-NH_2 and Mn-SBA-15-NH_2
442 together with theoretical curves calculated using LDFA and PDM models (experimental
443 conditions: 0.01 g adsorbent dose in 50 ml of 50 mg/L Cu solution at pH 5)
444

445 Table 5. Adsorption kinetic parameters of SBA-15-NH_2 and Mn-SBA-15-NH_2 (LDFA and
446 PDM models)

Adsorbents	k_f	D_s	D_p
	m/sec	m^2/sec	m^2/sec
SBA-15-NH_2	5.35×10^{-5}	2.50×10^{-10}	2.50×10^{-8}
Mn-SBA-15-NH_2	8.90×10^{-6}	7.60×10^{-12}	1.75×10^{-8}

447
448 3.2.3. Adsorption and desorption cycle experiment
449 The regenerative capacity of SBA-15-NH_2 and Mn-SBA-15-NH_2 was experimentally

evaluated after multiple cycles of adsorption and desorption (Fig. 10). Cu was desorbed from the exhausted adsorbents using acid (HCl) followed by alkaline (NaOH) regeneration. Cu desorption by acid is attributed to the detachment of Cu from amine group in acidic condition. This is reflected by the pH evaluation (Fig. 5) which showed near zero Cu adsorption occurred between pH 1-2. During the 10 times of adsorption and desorption cycle experiments, the adsorption capacity of SBA-15-NH_2 and Mn-SBA-15-NH_2 for Cu were stable with only minimal fluctuations, enabling to maintain more than 90% of the initial adsorption capacity of Cu. The results established the feasibility of high regenerative capacity of both the adsorbents.

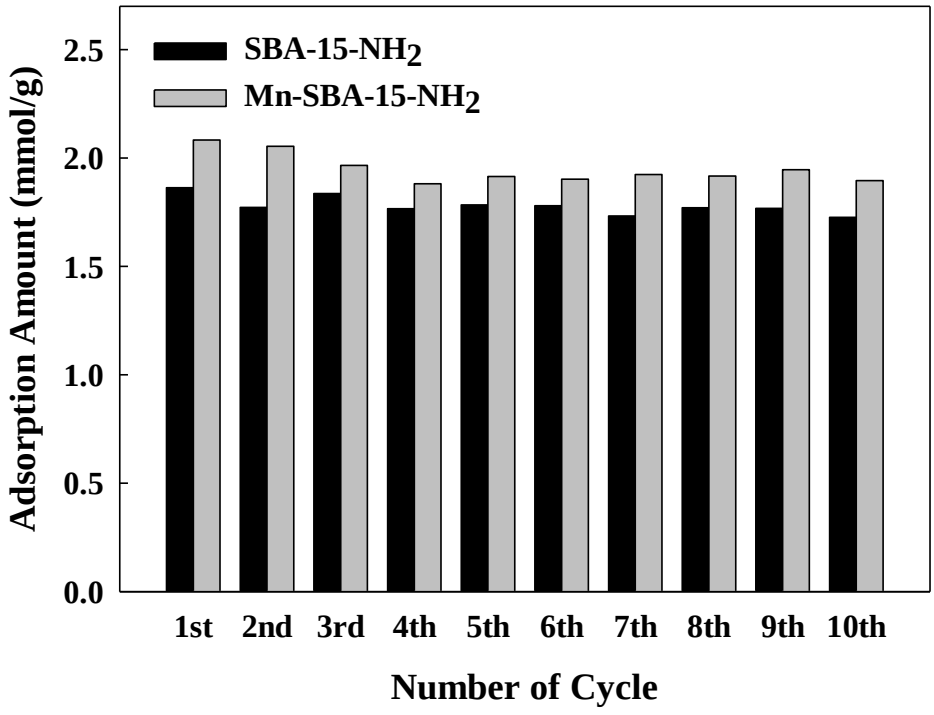

Fig. 10. Repeated Cu adsorption on SBA-15-NH_2 and Mn-SBA-15-NH_2 during adsorption-desorption experiment (experimental conditions: 0.2 g/L adsorbent dose in 300 mg/L of Cu

463 solution, pH = 5, equilibrium time: 24 h)

464 4. Conclusion

465 SBA-15, a 2D-hexagonal structured mesoporous silica material, was synthesized with
466 hydrothermal reaction, and subsequently modified by manganese loading and amine grafting,
467 to produce SBA-15-NH_2 and Mn-SBA-15-NH_2. Detailed physical and chemical analyses
468 were made to determine the crystal structure, chemical and surface morphology and surface
469 area and pore size of the synthesized SBA-15-NH_2 and Mn-SBA-15-NH_2. The selective Cu
470 adsorption capacity on SBA-15-NH_2 and Mn-SBA-15-NH_2 was evaluated. The results
471 showed that:

472 • The modified adsorbents SBA-15-NH_2 and Mn-SBA-15-NH_2 resulted in 3 – 9 times
473 higher adsorption capacity of heavy metals (Cu, Zn, Ni and Mn) compared to SBA-15

474 • Adsorption of heavy metals with both SBA-15-NH_2 and Mn-SBA-15-NH_2 were
475 satisfactorily fitted with Langmuir and Freundlich isotherm equations at optimum pH of
476 5. Mn-SBA-15-NH_2 achieved higher adsorption capacity of Cu (2.08 mmol/g), Zn (1.44
477 mmol/g), Ni (1.84 mmol/g) and Mn (1.28 mmol/g) than SBA-15-NH_2 (1.86, 1.26, 1.29
478 and 1.14 mmol/g).

479 • Mn-SBA-15-NH_2 exhibited high selective Cu adsorption (96% of the Cu single solution
480 adsorption capacity) in a mixed metal solution. This is attributed to the presence of
481 higher amine in Mn-SBA-15-NH_2 that formed strong chelating bonding with Cu
482 compared to other metals.

483 • Adsorption kinetic data were well fitted with LDFA and PDM models. The slower

484 diffusion rate of Mn-SBA-15-NH_2 compared to SBA-15-NH_2 was due to smaller pore
485 size upon manganese modification.

486 • Multiple cycle of adsorption and desorption experiments established the high
487 regenerative capacity of the modified adsorbent. Both SBA-15-NH_2 and Mn-SBA-15-
488 NH_2 were able to maintain 90% of Cu adsorption capacity even after 10 cycles of
489 adsorption and desorption experiments.

490

5. Reference

Aguado, J., Arsuaga, J.M., Arencibia, A., Lindo, M., Gascón, V., 2009. Aqueous heavy metals removal by adsorption on amine-functionalized mesoporous silica. J. Hazard. Mater. 163, 213-221.

Ali, R.M., Hamad, H.A., Hussein, M.M., Malash, G.F., 2016. Potential of using green adsorbent of heavy metal removal from aqueous solutions: Adsorption kinetics, isotherm, thermodynamic, mechanism and economic analysis. Ecol. Eng. 91, 317-332.

Anbia, M., Hariri, S.A., Ashrafizadeh, S.N., 2010. Adsorptive removal of anionic dyes by modified nanoporous silica SBA-3. Appl. Surf. Sci. 256, 3228-3233.

Anirudhan, T.S., Sreekumari, S.S., 2011. Adsorptive removal of heavy metal ions from industrial effluents using activated carbon derived from waste coconut buttons. J. Environ. Sci. 23, 1989-1998.

Benhamou, A., Basly, J.P., Baudu, M., Derriche, Z., Hamacha, R., 2013. Amino-functionalized MCM-41 and MCM-48 for the removal of chromate and arsenate. J. Colloid Interface Sci. 404, 135-9.

Cai, C., Zhao, M., Yu, Z., Rong, H., Zhang, C., 2019. Utilization of nanomaterials for in-situ remediation of heavy metal(loid) contaminated sediments: A review. Sci. Total Environ. 662, 205-217.

Calleja, G., Sanz, R., Arencibia, A., Sanz-Pérez, E.S., 2011. Influence of Drying Conditions on Amine-Functionalized SBA-15 as Adsorbent of CO2. Top. Catal. 54, 135-145.

Chang, F.-Y., Chao, K.-J., Cheng, H.-H., Tan, C.-S., 2009. Adsorption of CO2 onto amine-grafted mesoporous silicas. Sep. Purif. Technol. 70, 87-95.

Cui, J., Zhang, L., 2008. Metallurgical recovery of metals from electronic waste: A review. J.

514 Hazard. Mater. 158, 228-256.
515 Da'na, E., Sayari, A., 2012. Adsorption of heavy metals on amine-functionalized SBA-15
516 prepared by co-condensation: Applications to real water samples. Desalination 285,
517 62-67.
518 Da'na, E., De Silva, N., Sayari, A., 2011. Adsorption of copper on amine-functionalized
519 SBA-15 prepared by co-condensation: Kinetics properties. Chem. Eng. J. 166, 454-
520 459.
521 Da'na, E., Sayari, A., 2011. Adsorption of copper on amine-functionalized SBA-15 prepared
522 by co-condensation: Equilibrium properties. Chem. Eng. J. 166, 445-453.
523 Ezzeddine, Z., Batonneau-Gener, I., Pouilloux, Y., Hamad, H., Saad, Z., Kazpard, V., 2015.
524 Divalent heavy metals adsorption onto different types of EDTA-modified mesoporous
525 materials: Effectiveness and complexation rate. Microporous Mesoporous Mater. 212,
526 125-136.
527 Feng, G., Ma, J., Zhang, X., Zhang, Q., Xiao, Y., Ma, Q., et al., 2019. Magnetic natural
528 composite Fe3O4-chitosan@bentonite for removal of heavy metals from acid mine
529 drainage. J. Colloid Interface Sci. 538, 132-141.
530 Foo, K.Y., Hameed, B.H., 2010. Insights into the modeling of adsorption isotherm systems.
531 Chem. Eng. J. 156, 2-10.
532 Fu, F., Wang, Q., 2011. Removal of heavy metal ions from wastewaters: A review. J. Environ.
533 Manage. 92, 407-418.
534 Gao, Z., Wang, L., Qi, T., Chu, J., Zhang, Y., 2007. Synthesis, characterization, and
535 cadmium(II) uptake of iminodiacetic acid-modified mesoporous SBA-15. Colloids
536 Surf., A 304, 77-81.

537 Glöser, S., Tercero Espinoza, L., Gandenberger, C., Faulstich, M., 2015. Raw material
538 criticality in the context of classical risk assessment. Resour. Policy 44, 35-46.
539 Gonzales, R.r., Hong, Y., Park, J.-H., Kumar, G., Kim, S.-H., 2016. Kinetics and equilibria of
540 5-hydroxymethylfurfural (5-HMF) sequestration from algal hydrolyzate using
541 granular activated carbon. J. Chem. Technol. Biotechno. 91, 1157-1163.
542 Hadi, P., Xu, M., Lin, C.S.K., Hui, C.-W., McKay, G., 2015. Waste printed circuit board
543 recycling techniques and product utilization. J. Hazard. Mater. 283, 234-243.
544 Hariharan, G., Ponnusami, V., Srikanth, R., 2012. Wavelet method to film-pore diffusion
545 model for methylene blue adsorption onto plant leaf powders. J. Math. Chem. 50,
546 2775-2785.
547 Hernández-Morales, V., Nava, R., Acosta-Silva, Y.J., Macías-Sánchez, S.A., Pérez-Bueno,
548 J.J., Pawelec, B., 2012. Adsorption of lead (II) on SBA-15 mesoporous molecular
549 sieve functionalized with –NH2 groups. Microporous Mesoporous Mater. 160, 133-
550 142.
551 Jalali, M., Moradi, F., 2013. Competitive sorption of Cd, Cu, Mn, Ni, Pb and Zn in polluted
552 and unpolluted calcareous soils. Environ. Monit. Assess. 185, 8831-8846.
553 Jiang, Y., Gao, Q., Yu, H., Chen, Y., Deng, F., 2007. Intensively competitive adsorption for
554 heavy metal ions by PAMAM-SBA-15 and EDTA-PAMAM-SBA-15 inorganic–
555 organic hybrid materials. Microporous Mesoporous Mater. 103, 316-324.
556 Kim, J.Y., Balathanigaimani, M.S., Moon, H., 2015. Adsorptive Removal of Nitrate and
557 Phosphate Using MCM-48, SBA-15, Chitosan, and Volcanic Pumice. Water Air Soil
558 Pollut. 226, 431.
559 Kim, S.-H., Ngo, H.H., Shon, H.K., Vigneswaran, S., 2008. Adsorption and photocatalysis

560 kinetics of herbicide onto titanium oxide and powdered activated carbon. Sep. Purif.
561 Technol. 58, 335-342.
562 Kim, Y., Bae, J., Park, J., Suh, J., Lee, S., Park, H., et al., 2014. Removal of 12 selected
563 pharmaceuticals by granular mesoporous silica SBA-15 in aqueous phase. Chem. Eng.
564 J. 256, 475-485.
565 Koong, L.F., Lam, K.F., Barford, J., McKay, G., 2013. A comparative study on selective
566 adsorption of metal ions using aminated adsorbents. J. Colloid Interface Sci. 395, 230-
567 40.
568 Lee, J.-Y., Chen, C.-H., Cheng, S., Li, H.-Y., 2016. Adsorption of Pb(II) and Cu(II) metal ions
569 on functionalized large-pore mesoporous silica. Int. J. Environ. Sci. Technol. 13, 65-
570 76.
571 Lei, D., Zheng, Q., Wang, Y., Wang, H., 2015. Preparation and evaluation of aminopropyl-
572 functionalized manganese-loaded SBA-15 for copper removal from aqueous solution.
573 J. Environ. Sci. (China) 28, 118-27.
574 Li, J., Qi, T., Wang, L., Liu, C., Zhang, Y., 2007. Synthesis and characterization of imidazole-
575 functionalized SBA-15 as an adsorbent of hexavalent chromium. Mater. Lett. 61,
576 3197-3200.
577 Liang, Z., Shi, W., Zhao, Z., Sun, T., Cui, F., 2017. The retained templates as “helpers” for the
578 spherical meso-silica in adsorption of heavy metals and impacts of solution chemistry.
579 J. Colloid Interface Sci. 496, 382-390.
580 Liu, C., Bai, R., San Ly, Q., 2008. Selective removal of copper and lead ions by
581 diethylenetriamine-functionalized adsorbent: Behaviors and mechanisms. Water Res.
582 42, 1511-1522.

583 Lombardo, M.V., Videla, M., Calvo, A., Requejo, F.G., Soler-Illia, G.J.A.A., 2012.
584 Aminopropyl-modified mesoporous silica SBA-15 as recovery agents of Cu(II)-
585 sulfate solutions: Adsorption efficiency, functional stability and reusability aspects. J.
586 Hazard. Mater. 223-224, 53-62.
587 McManamon, C., Burke, A.M., Holmes, J.D., Morris, M.A., 2012. Amine-functionalised
588 SBA-15 of tailored pore size for heavy metal adsorption. J. Colloid Interface Sci. 369,
589 330-337.
590 Mureseanu, M., Reiss, A., Stefanescu, I., David, E., Parvulescu, V., Renard, G., et al., 2008.
591 Modified SBA-15 mesoporous silica for heavy metal ions remediation. Chemosphere
592 73, 1499-504.
593 Nagajyoti, P.C., Lee, K.D., Sreekanth, T.V.M., 2010. Heavy metals, occurrence and toxicity
594 for plants: a review. Environ. Chem. Lett. 8, 199-216.
595 Naidu, G., Ryu, S., Thiruvenkatachari, R., Choi, Y., Jeong, S., Vigneswaran, S., 2019. A
596 critical review on remediation, reuse, and resource recovery from acid mine drainage.
597 Environ. Pollut. 247, 1110-1124.
598 Niu, X., Li, Y., 2007. Treatment of waste printed wire boards in electronic waste for safe
599 disposal. J. Hazard. Mater. 145, 410-416.
600 Özdemir, S., Kilinc, E., Poli, A., Nicolaus, B., Güven, K., 2009. Biosorption of Cd, Cu, Ni,
601 Mn and Zn from aqueous solutions by thermophilic bacteria, Geobacillus toebii
602 sub.sp. decanicus and Geobacillus thermoleovorans sub.sp. stromboliensis:
603 Equilibrium, kinetic and thermodynamic studies. Chem. Eng. J. 152, 195-206.
604 Popuri, S.R., Vijaya, Y., Boddu, V.M., Abburi, K., 2009. Adsorptive removal of copper and
605 nickel ions from water using chitosan coated PVC beads. Bioresour. Technol. 100,

194-199.

Ryu, S., Naidu, G., Hasan Johir, M.A., Choi, Y., Jeong, S., Vigneswaran, S., 2019. Acid mine drainage treatment by integrated submerged membrane distillation–sorption system. Chemosphere 218, 955-965.

Ryu, S.C., Kim, J.Y., Hwang, M.J., Moon, H., 2018. Recovery of nitrate from water streams using amine-grafted and magnetized SBA-15. Korean J. Chem. Eng. 35, 489-497.

Saad, R., Hamoudi, S., Belkacemi, K., 2007. Adsorption of phosphate and nitrate anions on ammonium-functionnalized mesoporous silicas. J. Porous Mater. 15, 315-323.

Saikia, L., Srinivas, D., 2009. Redox and selective oxidation properties of Mn complexes grafted on SBA-15. Catal. Today 141, 66-71.

Saikia, L., Srinivas, D., Ratnasamy, P., 2007. Comparative catalytic activity of Mn(Salen) complexes grafted on SBA-15 functionalized with amine, thiol and sulfonic acid groups for selective aerial oxidation of limonene. Microporous Mesoporous Mater. 104, 225-235.

Šćiban, M., Radetić, B., Kevrešan, Ž., Klašnja, M., 2007. Adsorption of heavy metals from electroplating wastewater by wood sawdust. Bioresour. Technol. 98, 402-409.

Shahbazi, A., Younesi, H., Badiei, A., 2011. Functionalized SBA-15 mesoporous silica by melamine-based dendrimer amines for adsorptive characteristics of Pb(II), Cu(II) and Cd(II) heavy metal ions in batch and fixed bed column. Chem. Eng. J. 168, 505-518.

Singh, R.P., Agrawal, M., 2007. Effects of sewage sludge amendment on heavy metal accumulation and consequent responses of Beta vulgaris plants. Chemosphere 67, 2229-2240.

Sreenu, B., Sharma, P., Seshaiah, K., Singh, A.P., 2016. Synthesis and characterization of

629 nanoporous silica SBA-15 diaminocyclohexane and its application in removal of
630 Cu(II) and Ni(II) from aqueous solution. Desalin. Water Treat. 57, 15397-15409.
631 Szegedi, A., Popova, M., Goshev, I., Mihály, J., 2011. Effect of amine functionalization of
632 spherical MCM-41 and SBA-15 on controlled drug release. J. Solid State Chem. 184,
633 1201-1207.
634 Wang, S., Wang, K., Dai, C., Shi, H., Li, J., 2015. Adsorption of Pb2+ on amino-
635 functionalized core–shell magnetic mesoporous SBA-15 silica composite. Chem. Eng.
636 J. 262, 897-903.
637 Wei, Q., Nie, Z.-R., Hao, Y.-L., Liu, L., Chen, Z.-X., Zou, J.-X., 2006. Effect of synthesis
638 conditions on the mesoscopical order of mesoporous silica SBA-15 functionalized by
639 amino groups. J. Sol-Gel Sci. Technol. 39, 103-109.
640 Xiao, F., Cheng, J., Cao, W., Yang, C., Chen, J., Luo, Z., 2019. Removal of heavy metals
641 from aqueous solution using chitosan-combined magnetic biochars. J. Colloid
642 Interface Sci. 540, 579-584.
643 Xue, M., Yang, Y., Ruan, J., Xu, Z., 2012. Assessment of Noise and Heavy Metals (Cr, Cu,
644 Cd, Pb) in the Ambience of the Production Line for Recycling Waste Printed Circuit
645 Boards. Environ. Sci. Technol. 46, 494-499.
646 Yan, X., Zhang, L., Zhang, Y., Yang, G., Yan, Z., 2011. Amine-Modified SBA-15: Effect of
647 Pore Structure on the Performance for CO2 Capture. Ind. Eng. Chem. Res. 50, 3220-
648 3226.
649 Yavuz, M., Gode, F., Pehlivan, E., Ozmert, S., Sharma, Y.C., 2008. An economic removal of
650 Cu2+ and Cr3+ on the new adsorbents: Pumice and polyacrylonitrile/pumice
651 composite. Chem. Eng. J. 137, 453-461.

652 Yokoi, T., Yoshitake, H., Yamada, T., Kubota, Y., Tatsumi, T., 2006. Amino-functionalized
653 mesoporous silica synthesized by an anionic surfactant templating route. J. Mater.
654 Chem. 16, 1125.
655 Yu, M., Li, Z., Xia, Q., Xi, H., Wang, S., 2007. Desorption activation energy of
656 dibenzothiophene on the activated carbons modified by different metal salt solutions.
657 Chem. Eng. J. 132, 233-239.
658 Zhao, K., Liu, S., Wu, Y., Lv, K., Yuan, H., He, Z., 2015. Long Cycling Life Supercapacitors
659 Electrode Materials: Ultrathin Manganese Dioxide Nanoscrolls Adhered to Graphene
660 by Electrostatic Self-Assembly. Electrochim. Acta 174, 1234-1243.
661 Zhao, Q., Guo, F., Zhang, Y., Ma, S., Jia, X., Meng, W., 2017. How sulfate-rich mine
662 drainage affected aquatic ecosystem degradation in northeastern China, and potential
663 ecological risk. Sci. Total Environ. 609, 1093-1102.
664 Zhu, J., He, J., 2012. Facile Synthesis of Graphene-Wrapped Honeycomb MnO2
665 Nanospheres and Their Application in Supercapacitors. ACS App. Mat. Interfaces 4,
666 1770-1776.
667 Zucchetto, N., Reber, M.J., Pestalozzi, L., Schmid, R., Neels, A., Brühwiler, D., 2018. The
668 structure of mesoporous silica obtained by pseudomorphic transformation of SBA-15
669 and SBA-16. Microporous Mesoporous Mater. 257, 232-240.

670